

# Chemical and physical properties of plumes of anthropogenic pollutants transported over the North Atlantic during the North Atlantic Regional Experiment

P. H. Daum,<sup>1</sup> L. I. Kleinman,<sup>1</sup> L. Newman,<sup>1</sup> W. T. Luke,<sup>2</sup>  
J. Weinstein-Lloyd,<sup>3</sup> C. M. Berkowitz,<sup>4</sup>  
and K. M. Busness<sup>4</sup>

**Abstract.** Plumes of photochemical pollutants transported from the industrialized regions of the northeast United States and Canada were sampled over the North Atlantic Ocean at distances up to 1000 km from the coast. The plumes were found in well defined layers up to 1 km thick and were usually isolated from the surface by a low altitude inversion. Plume composition was consistent with the occurrence of extensive photochemical processing during transit from source regions as indicated by high O<sub>3</sub> concentrations (O<sub>3</sub> maximum ~150 parts per billion by volume (ppbv)), generally high fractional conversion (>85%) of NO<sub>x</sub> to its oxidation products, and high peroxide concentrations (median 3.6 ppbv; maximum 11 ppbv). These observations are in accord with processing times estimated from back trajectory analysis. CO and O<sub>3</sub> concentrations were well correlated ( $r^2 = 0.64$ ) with a slope (0.26) similar to previous measurements in photochemically aged air. Good correlations were also observed between CO and accumulation mode particle number densities ( $r^2 = 0.64$ ), and CO and NO<sub>y</sub> ( $r^2 = 0.67$ ). O<sub>3</sub> was found to depend nonlinearly on the NO<sub>x</sub> oxidation product concentration. At low values of (NO<sub>y</sub>-NO<sub>x</sub>), the slope (14) was within the range of values measured previously in photochemically aged air masses, at higher concentrations the slope was much lower (4.6). The low slope at high concentrations is attributed to minimization of losses of NO<sub>x</sub> oxidation products in spatially well-defined plumes during transport. A strong linear correlation ( $r^2 = 0.73$ ) was found between O<sub>3</sub>, and the concentration of radical sink species as represented by the quantity (NO<sub>y</sub>-NO<sub>x</sub>) + 2H<sub>2</sub>O<sub>2</sub>.

## 1. Introduction

The North Atlantic Regional Experiment (NARE) was conducted during the late summer 1993 to investigate the chemical and transport processes that determine the distribution of O<sub>3</sub> and related pollutants over the Western North Atlantic Ocean (WNAO). This large-scale experiment focused on measurement of O<sub>3</sub>, O<sub>3</sub> precursors, and tracers of anthropogenic emissions. The experiment was motivated by evidence from recent observational [Parrish *et al.*, 1993a; Anderson *et al.*, 1993; Galloway *et al.*, 1984] and modeling studies [e.g., Fishman *et al.*, 1985] that emissions from sources in North America can travel long distances and may adversely affect environmental quality of the WNAO. Potential effects include alteration of the capacity of the maritime atmosphere to remove trace substances by oxidation reactions [Isaksen and Hov, 1987; Thompson *et al.*, 1989], changes in planetary albedo because of backscatter from anthropogenic aerosol particles [Charlson *et al.*, 1991] or through modification of the size distribution of

cloud droplets [Schwartz, 1988], and alteration of marine productivity through deposition of nutrients to the ocean surface.

The basic strategy of the summer 1993 NARE was to use aircraft and a series of surface sites to track the chemical transformations and the vertical and horizontal dispersion of air masses containing pollutants as they were transported off the east coast of North America. Measurements in the western North Atlantic were centered in an area roughly bounded on the west by the east coast of North America, and on the east by Sable Island (~44°N latitude, 60°W longitude); north-south boundaries were roughly between 42°N and 45°N latitude. These measurements were augmented by measurements of O<sub>3</sub> at several sites on the west coast of Europe, and the British Isles, by measurements of O<sub>3</sub>, CO and related species in the Azores, and by several flights of the British Meteorological Flight Service C-130 aircraft, two of which crossed the North Atlantic.

The three aircraft stationed in the western North Atlantic were placed at successively more easterly locations to sample air masses as they advected eastward from the North American continent. The King Air aircraft, instrumented by the National Center for Atmospheric Research and the Aeronomy Laboratory of the National Oceanic and Atmospheric Administration and stationed in Portland, Maine, principally sampled air masses in the region nearest the North American coast when emissions were relatively fresh. The Institute of Aerospace Research/Atmospheric Environment Service of Canada Twin Otter aircraft sampled principally in the vicinity of Yarmouth, Nova Scotia, about 500 km downwind of the major source regions in the northeastern United States. The Department of Energy (DOE) Gulfstream G-1 aircraft based in Halifax, Nova Scotia, generally sampled air masses east of Nova Scotia, 800-

<sup>1</sup>Environmental Chemistry Division, Department of Applied Science, Brookhaven National Laboratory, Upton, New York.

<sup>2</sup>Air Resources Laboratory, National Oceanic and Atmospheric Administration, Silver Spring, Maryland.

<sup>3</sup>Chemistry/Physics Department, SUNY Old Westbury, Old Westbury, New York.

<sup>4</sup>Battelle Pacific Northwest Laboratory, Richland, Washington.

1000 km downwind of the source regions. These sampling locales corresponded to estimated transport times from the Boston metropolitan area of <1 day, 1–2 days, and 2–4 days, respectively. Aircraft measurements were supported by continuous measurements at surface sites in southern Nova Scotia (Chebogue Point) and at Sable Island, about 250 km east-southeast, of Halifax.

Here we report measurements made by the DOE G-1 aircraft of the chemical properties, and physical disposition of plumes of photochemical pollutants advected out over the North Atlantic from the northeastern United States source regions during the program. Because of the location of the G-1 operational region well downwind of sources, these plumes were typically well aged photochemically, having not been exposed to fresh emissions for periods of 24 hours or more. The plumes were found to have high  $O_3$  concentrations and high concentrations of photochemical product species. The purpose of this paper is to examine the chemical properties of these plumes, to compare them to equivalent measurements made at other locations, and to examine aspects of the combined transport/transformation process that led to the unusual accumulation of photochemical product species.

## 2. Experimental

### 2.1. Instrumentation

Measurements were conducted with the DOE Gulfstream G-1 aircraft, an intermediate-sized, twin-turboprop aircraft equipped with an array of scientific instrumentation for measurement of trace gas and aerosol concentrations. The capabilities of this aircraft have recently been described [Spicer *et al.*, 1994]. Description of instrument systems relevant to the data discussed here are given below.

Ambient air samples were provided by externally mounted inlets on the right forward section of the fuselage. Two 2.5-cm diameter inlets provided sample air for the filter collection systems on the port side of the aircraft forward of the engines. Multiple inlets on the forward starboard side of the aircraft supplied sample air for trace gas analysis. All sample lines and manifolds were either Teflon or Teflon-lined to minimize losses of trace species. Two PMS probes (Particle Measurement Systems, Boulder, Colorado), a forward-scattering aerosol spectrometer probe (FSSP), and an axial-scattering aerosol spectrometer probe (ASASP) for measuring aerosol number concentrations and size distributions ( $0.2 < d < 47 \mu\text{m}$ ) were mounted on either side of the aircraft nose. An Eppley pyranometer for measuring total solar UV irradiance was mounted on the top of the aircraft fuselage. Atmospheric state parameters (dew point, temperature, and pressure) were measured using the standard G-1 instruments [Spicer *et al.*, 1994]. Position was determined continuously from LORAN and GPS navigation systems.

Aerosol composition and mass concentrations, and gaseous  $HNO_3$  and  $SO_2$  concentrations were measured using a filter pack system consisting of a quartz filter for aerosol collection followed by a NaCl-impregnated cellulose filter for collection of  $HNO_3$ , and a  $K_2CO_3$ /glycerol-impregnated filter for collection of  $SO_2$ . Filters were mounted in 47-mm-diameter polycarbonate filter holders. "Filter packs" were loaded prior to each flight and immediately unloaded and stored upon termination of each flight. The exposed filters were packaged in sealed individual polyethylene bags. Upon arrival at the laboratory, filters were stored below  $0^\circ\text{C}$  prior to analysis. Procedures for the preparation, collection, and analysis of these filters, and specification

of uncertainties are given by Daum and Leahy [1985]. Filters were collected for time periods that ranged between 15 and 50 min depending on conditions.

Peroxide concentrations were determined using a two-channel continuous flow analyzer [Lazrus *et al.*, 1985] which had been adapted to permit peroxide determination by the recently developed non-enzymatic method [Lee *et al.*, 1990, 1994]. To date, only  $H_2O_2$ , methyl hydroperoxide (MHP) and hydroxymethyl hydroperoxide (HMHP) have been detected in scrubbed ambient air [Hellpointer *et al.*, 1989; Ilewitt and Kok, 1991]. Because ground measurements at Chebogue Point using a three-channel peroxide analyzer indicated no significant concentrations of HMHP, the aircraft instrument was configured to measure  $H_2O_2$  and MHP. P-hydroxyphenylacetic acid (pOHPAA) and Fe(II)-benzoic acid (FeBA) reagents were used in the two channels for determining total peroxides and hydrogen peroxide in channels A and B, respectively. Air was scrubbed into pH 9 stripping solution, resulting in the rapid hydrolysis of any ambient HMHP into  $H_2O_2$ ; thus the difference between channels A and B, after correction for MHP scrubbing efficiency, gave the concentration of MHP. Deriving concentrations by this method assumes the existence of only  $H_2O_2$ , MHP, and HMHP. The detection limit of the measurement, based on 3 times the standard deviation of noise on the zero air baseline, is 78 pptv. Uncertainty in determining MHP was assessed by comparing the response of FeBA reagent in channels A and B to a common air sample during a one hour time period. This analysis gave a detection limit of 300 parts per trillion by volume (pptv), based on 3 times the difference between the response difference between the two channels. The instrument was calibrated using aqueous phase standards obtained by dilution of stock solution of  $H_2O_2$ . The concentration of the  $H_2O_2$  stock solution was determined by titration with standardized permanganate solution.

$NO_y$  measurements ( $NO$ ,  $NO_x$  and  $NO_y$ ) were made with a two-channel  $O_3$  chemiluminescent NO detector similar to the one described by Kleinman *et al.* [1994], with the exception of the addition of  $200 \text{ cm}^3/\text{min}$  of  $O_2$  saturated with water vapor to the inlet to minimize response changes of the instrument due to changes in relative humidity. During the present program one of the two instrument channels was devoted exclusively to the measurement of  $NO_y$ ; the second channel was manually switched between  $NO$  and  $NO_x$ . The  $NO_x$  channel utilized a photolytic converter with an efficiency of 48.5%.  $NO_y$  was determined using a hot ( $350^\circ\text{C}$ ) molybdenum converter (efficiency >95%). The efficiencies of both the photolytic and molybdenum converters were periodically determined using an  $NO_2$  permeation source diluted with zero air. Instrument response was determined by multipoint calibrations at the surface, and by standard addition of a high concentration of  $NO$  (~90 ppbv) in flight. In-flight instrument zeroes were performed by mixing ambient air with ozone in a prereaction chamber. Sample air for the  $NO_y$  instrument was provided by ram air inlet consisting of approximately 1.5 m of 1.25-cm ID Teflon tubing vented at the back of the instrument. It is estimated that the residence time of sample air in this inlet was between 30 and 50 ms (i.e., between 30 and 50% of the free stream velocity). Based upon variations of instrument zero response and response to in-flight standard additions, the uncertainty in measurement of the  $NO$  concentration for 10 s averaged data is estimated to be  $30 \text{ ppt} + 15\%$  of the  $NO$  concentration and for  $NO_y$  is estimated to be  $50 \text{ ppt} + 15\%$  of the  $NO_y$  concentration. The quantity reported here as " $NO_x$ " was calculated as the quotient of the  $NO_x$  channel output and the photolytic converter efficiency. Since the photolytic converter efficiency is ~50%, " $NO_x$ " is

approximately equal to  $\text{NO}_2 + 2\text{NO}$ , which overestimates the actual  $\text{NO}_x$  concentration by the NO concentration. However, since the NO concentration was typically much smaller than " $\text{NO}_x$ " ( $\text{NO} < 0.25\text{NO}_x$ ) in adjacent measurements, we estimate that the positive bias in the  $\text{NO}_x$  concentrations is at most on the order of 20%; in many cases the bias appears to be much lower. This bias does not influence our conclusions regarding the small fractional quantity of  $\text{NO}_y$  present as  $\text{NO}_x$  nor does it influence our analysis of the relationship between  $(\text{NO}_y - \text{NO}_x)$  and  $\text{O}_3$ , or between the quantity  $\{(\text{NO}_y - \text{NO}_x) + 2\text{H}_2\text{O}_2\}$  and  $\text{O}_3$ .

Ozone was measured using a UV absorption instrument (Thermo Electron Corporation, model 49) with an estimated uncertainty of 5%.  $\text{SO}_2$  was measured by pulsed fluorescence (Thermo Electron Corporation, Model 43S) with a detection limit of 100 ppt and a time response of 2 min. CO was measured using a nondispersive infrared detector (Thermo Electron model 48) that had been modified according to the design of *Dickerson and Delany* [1988]. The instrument was calibrated using a National Institute of Standards and Technology transfer standard. Instrument uncertainty for the 1-min averaged data reported here is estimated to be 30 ppb + 15% of the measured concentration.

## 2.2. Meteorological Conditions

A description of the daily meteorological conditions over the study period is given in Table 1. A more detailed analysis of the synoptic patterns associated with photochemical plumes over the WNAO during this study is given by *Berkowitz et al.* [this issue].

Between August 12 and August 24, meteorological conditions were characterized by light and variable winds associated with high pressure over the sampling domain. This anticyclonic pattern weakened on August 14–15, but redeveloped on August 16, and persisted through August 20. Although such systems are generally associated with pollutant buildup over continental source regions, the light winds and weak mixing in the project region were not conducive to transport of pollutants from the North American continent to the sampling area. This is consistent with low concentrations of pollutants measured on flights between August 12 and 24, Table 2.

A series of fronts began to move through the area on August 20, with periods of high pressure alternating with periods of cyclonic flow. The most clearly defined pollutant layers in the western North Atlantic were found to be associated with the air masses preceding these eastward moving cyclones [*Berkowitz et al.*, this issue]. Apparently these systems have an organized circulation of sufficient duration and spatial extent to transport material from the east coast of North America throughout the sampling domain. As seen in Table 2, this pattern characterized days when the highest pollutant concentrations were observed.

## 2.3. Flight Summary

The G-1 flew 13 missions during the summer 1993 NARE program. The general location of these flights and a brief summary of the conditions under which the flights were conducted is given in Table 2. The flights consisted of combinations of vertical soundings to determine the thermodynamic structure of the atmosphere and to locate layers of transported pollutants and horizontal transects to establish the horizontal extent of any pollutant layers that were identified. Vertical profiles typically extended from within 100 m of the surface to altitudes of 3–5 km, and horizontal fixed altitude legs extended

Table 1. Synoptic Conditions

Date	Synoptic Description
August 12	Region had been under influence of surface high pressure for 3 days; winds light and variable, clear skies.
August 16	High pressure circulation moved out of the domain. Frontal passage on August 16, 0000 UTC, post-frontal air in region on August 16, 1200 UTC.
August 17	South edge of anticyclone over domain; winds light and variable at surface.
August 18	Southwesterly flow on west edge of domain in advance of cold front.
August 20	Anticyclonic flow from northeast.
August 22	High pressure over region with weak pressure gradients; light and variable winds from south/southeast.
August 23	Weak pressure gradient over region; light and variable winds.
August 24	Pre-frontal conditions with well defined cyclone flow from southwest.
August 25	Pre-frontal conditions. Flow not well-defined, but generally from southwest.
August 27	Pre-frontal conditions. Flow not well-defined, but generally from the southwest.
August 28	Pre-frontal conditions with well-defined cyclonic flow from southwest.
August 29	Post-frontal conditions; cyclonic flow from northwest.
August 31	Weak southerly flow in advance of a warm front.

for distances as long as several hundred kilometers, depending on conditions. A substantial number of flights sampled air in conjunction with surface measurements being made either at Chebogue Point or at Sable Island. Five flights were made to Sable Island specifically for the purpose of examining the relationship between air composition measured aloft and at the surface.

With the exception of a small number of flight segments, flights prior to August 24 were conducted in background air. In this context, background air is defined as air that had not recently been in contact with the boundary layer of a land mass with significant anthropogenic sources as indicated by back trajectories, radon concentrations, or both. Major transport events from the North American continent were sampled by the G-1 during flights on August 27, 28, and 31. On August 27, a major plume was sampled southwest of Nova Scotia; on August 28, a major plume was sampled to the east and southeast of Nova Scotia, a relatively widespread area of pollutants was sampled over the Bay of Fundy on August 31. These plumes exhibited  $\text{O}_3$  concentrations up to 150 ppbv,  $\text{NO}_y$  concentrations up to ~20 ppbv, and accumulation mode particle number densities that were as high as  $2500/\text{cm}^3$ .

## 2.4. Selection of Plume Data

There are many criteria (e.g., back trajectory analysis, radon concentration measurements, or other tracer measurements) which could be used to identify air recently exposed to regional sources of pollutants in the northeastern United States, and southeastern Canada. For the current analysis a pragmatic approach is adopted and the data are segregated according to the  $\text{NO}_y$  concentration. Thus all data collected under conditions when  $\text{NO}_y$  concentrations were in excess of 1 ppbv were selected for analysis. While it can be argued that using  $\text{NO}_y$  concentrations as a means of segregating plume from background data is inappropriate because of the relatively short lifetime of  $\text{NO}_y$  in the atmosphere, isolating the data in this way is consistent with the results of back trajectory analysis, and with

Table 2. Flight Summary

Date (Time, Ut)	Location	Conditions
August 12 (1900-2130)	Halifax-Chebogue Point and return	intercomparison flight; background.
August 16 (1500-1920)	Halifax-St. John NB, Princeton, ME- Yarmouth NS-Halifax	background
August 17 (1600-1845)	Halifax-Sable Island and return	background
August 18 (1500-1830)	Halifax-Sable Island and return	background
August 20 (1600-1945)	Halifax-St. John, NB-Princeton, ME- Chebogue Point-Halifax	background except for plume east of Princeton, ME, at coast.
August 22 (1500-1720)	Halifax-Sable Island and return	background
August 23 (1800-2200)	Halifax-Princeton, ME-Chebogue Point- Halifax	background
August 24 (1330-1700)	Halifax-Bay of Fundy-Chebogue Point- Halifax	moderately polluted conditions over Bay of Fundy.
August 25 (1100-1500)	South and east of Halifax; profile at Sable Island	polluted layer 500-1500 m.
August 27 (1345-1750)	Halifax-Chebogue Point-42°N/68°W and Return	extensive polluted layer < 150 m south of NS; O <sub>3</sub> ~150 ppb, NO <sub>y</sub> ~15 ppbv.
August 28 (1325-1745)	Southeast of Halifax to 44°N/62°W then south to 42°N/62°W and return	high concentrations of pollutants 400-2,000 m; O <sub>3</sub> ~150 ppb, NO <sub>y</sub> ~15ppb.
August 29 (1330-1615)	Southeast & east of Halifax	generally polluted, plumes not well defined.
August 31 (1530-1945)	Halifax-Princeton, ME-Chebogue Point- Halifax	generally polluted, plumes not well defined.

other measures of anthropogenic influence such as CO concentration and accumulation mode aerosol particle number densities. Our subsequent analysis and interpretation below then refers only to data for which the NO<sub>y</sub> concentrations are >1 ppbv. Measurements thus segregated derive principally from the six flights made from August 24 through 31, 1993.

### 3. Results and Discussion

#### 3.1. Location and Spatial Properties of Plumes

A map showing the distribution of flight tracks during which air containing [NO<sub>y</sub>] > 1 ppbv was encountered is given in Figure 1. Distances from major source regions on the United States east coast ranged from ~300 km to > 1000 km. On many flights these regions of high pollutant concentrations were traversed for distances up to several hundred kilometers; in many instances these regions were thought to extend, on the basis of back trajectory analysis and meteorological conditions, over areas much larger than were actually sampled.

Plumes were typically encountered at relatively low altitudes (<1.5 km) and were most often present in isolated layers. The former is illustrated by Figure 2. Figure 2a shows all of the NO<sub>y</sub> data collected during the entire program plotted as a function of altitude. It is clear from this plot, that not only are the NO<sub>y</sub> concentrations generally higher in the boundary layer (<2 km) than in the free troposphere, but also that most of the extreme concentrations occur at low altitudes; for example there are few instances for which the NO<sub>y</sub> concentration is >1 ppbv above 2 km, whereas below 2 km, 60% of the measurements are in excess of 1 ppbv. Thus, while there is some evidence for transport of relatively fresh emissions at higher altitudes, this is not a prominent feature of our data. The observation of extensive regions of pollutants near the ocean surface (< 200 m) was also not common.

Figure 2b shows an altitude profile of all of the O<sub>3</sub> data for which NO<sub>y</sub> < 1 ppbv; Figure 2c shows the O<sub>3</sub> data for which NO<sub>y</sub> > 1 ppbv. It is clear from this figure that higher O<sub>3</sub> concentrations are associated with NO<sub>y</sub> > 1 ppbv. (The dependency of O<sub>3</sub> on NO<sub>y</sub> will be examined in a subsequent section). This association is consistent with O<sub>3</sub> formation chemistry wherein NO<sub>x</sub> serves as a catalyst for O<sub>3</sub> generation. Note that in Figure 2b, which may be considered to represent background conditions, that O<sub>3</sub> decreases with increasing altitude. Indeed, the lowest O<sub>3</sub> concentrations measured during the entire program were found at altitudes < 500 m. The generally lower O<sub>3</sub> concentrations near the ocean surface may reflect O<sub>3</sub> losses to the surface and/or that near-surface O<sub>3</sub> in this region originates from higher altitudes.

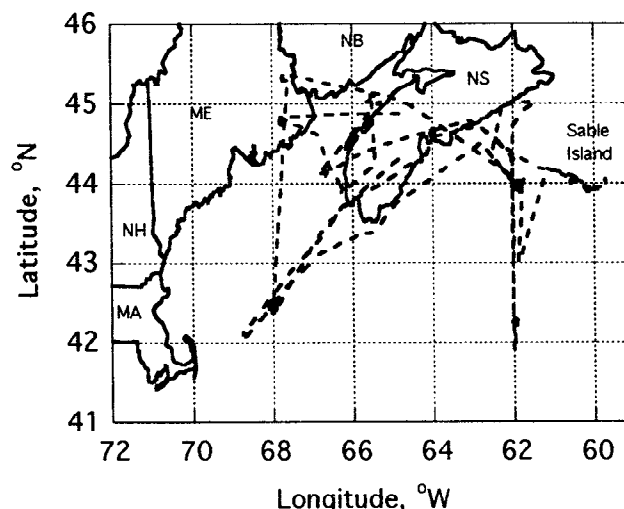


Figure 1. Map of project area showing flight tracks where NO<sub>y</sub> concentrations > 1 ppbv were sampled.

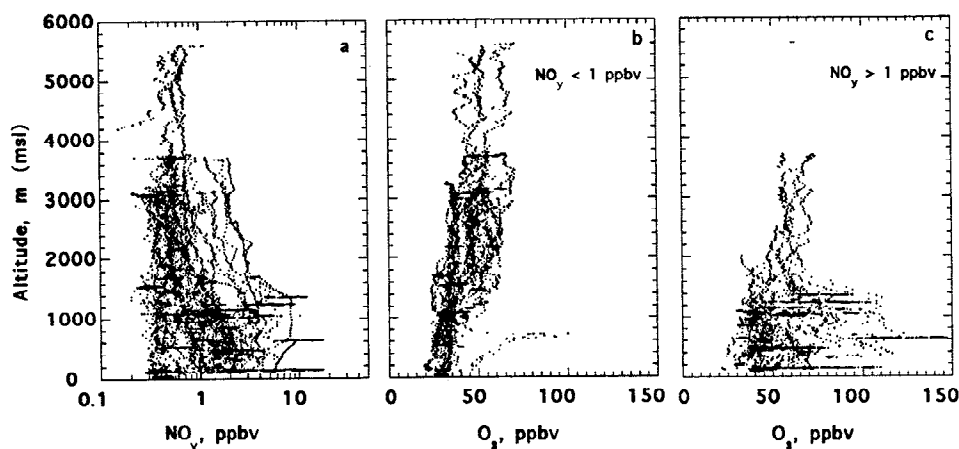


Figure 2. Vertical profiles respectively of all of the  $\text{NO}_y$ ,  $\text{O}_3$  for which  $\text{NO}_y < 1$  ppbv, and  $\text{O}_3$  for which  $\text{NO}_y > 1$  ppbv, measured by the G-1 during NARE.

To illustrate the horizontal and vertical structure of the plumes and some elements of their composition, data collected during flights made on August 27 and 28, 1993, through two of the most extensive and well-defined plumes sampled during the program are examined. Flight tracks associated with the plumes sampled on these two days are given in Figure 3. Back trajectories ending at altitudes corresponding to the horizontal transects discussed below are also shown. Synoptic conditions causing transport of these plumes to the North Atlantic were as follows. On August 27, a weak low pressure center was located over northeastern Minnesota with an associated coldfront extending south-southwest through Minnesota and Iowa. A weak high pressure center was located on the North Carolina/Virginia border. The combination of these two systems caused the surface flow along the northeast coast of the United States from central New Jersey through central Maine to be from the southwest. Between August 27 and 28, the low-pressure system intensified and moved rapidly to the northeast, and by early morning was centered over the province of Quebec with an associated cold front extending south-southwest through western New York and Ohio, and a warm front extending southeast from

central Quebec through the northern part of Nova Scotia. Flows along the northeast coast of the United States continued from the southwest.

The aircraft temperature/dew point sounding made on August 27, 1993, at the location indicated in Figure 3 is shown in Figure 4. This sounding exhibits a low-level temperature inversion with a top at circa 400 m, and two additional inversions at  $\sim 1500$  m and 3000 m. The temperature lapse rate derived from the sounding indicates neutral stability, and in combination with the aforementioned inversions, suggests that little mixing between layers had occurred. The dew point sounding, similar to the temperature sounding, exhibits three distinct macroscopic layers: a moist layer below the inversion at 1500 m, a somewhat dryer layer between the inversions at 1500 and 3000 m, and a very dry layer above 3000 m.

Back trajectories with end points at altitudes corresponding to the three principal layers in this profile indicate that air below the inversion at 1500 m had only recently ( $< 24$  hours) been transported from source rich regions in the vicinity of Boston, Massachusetts. In contrast, back trajectories calculated at 2300 and 3300 m suggest that air at these altitudes had not been in contact with source regions for extended periods of time. The back trajectories are consistent with  $\text{NO}_y$  and  $\text{O}_3$  concentrations measured during this sounding, Figure 4. Below 1500 m, both  $\text{NO}_y$  and  $\text{O}_3$  exhibit concentrations consistent with recent contact with source regions. Above 1500 m, the  $\text{NO}_y$  concentration decreases to quite small values;  $\text{O}_3$  decreases in the middle layer, but then increases in the upper layer. The latter may be an indication of a stratospheric source for  $\text{O}_3$ , or may be due to long-range transport of highly processed air that had been influenced by anthropogenic pollutants at some time in its history. Note also in Figure 4 the presence of a highly polluted layer at the very bottom of the profile.

Trace gas concentrations measured during an extended flight from the location of the spiral northeastward toward Nova Scotia are shown in Figure 5. This flight was made at an altitude of 130 - 150 m above the ocean surface in a layer of pollutants trapped within the low level inversion topping at 400 m (Figure 4). The back trajectory applicable to the southernmost portion of this transect (Figure 3) suggests that the air had been over northeastern Massachusetts only 6 hours prior to sampling. Concentrations are plotted as a function of latitude along the flight track (Figure 3). From the various panels in this figure, it is apparent that this low-level plume extended for a distance of at least 200 km. Trace gas concentrations (Figure 5) reached

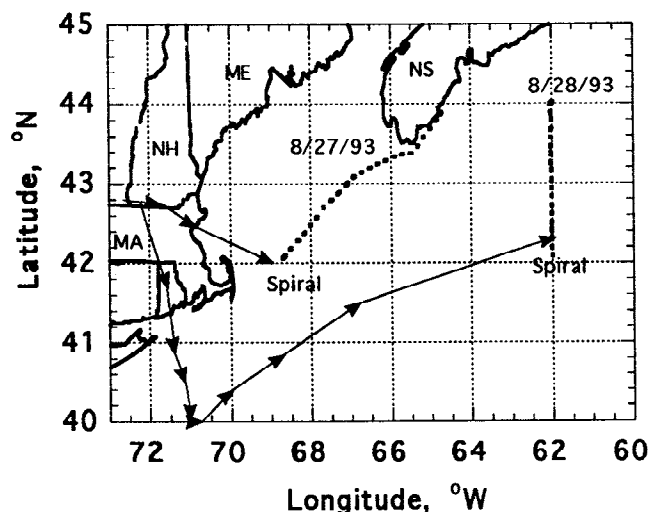
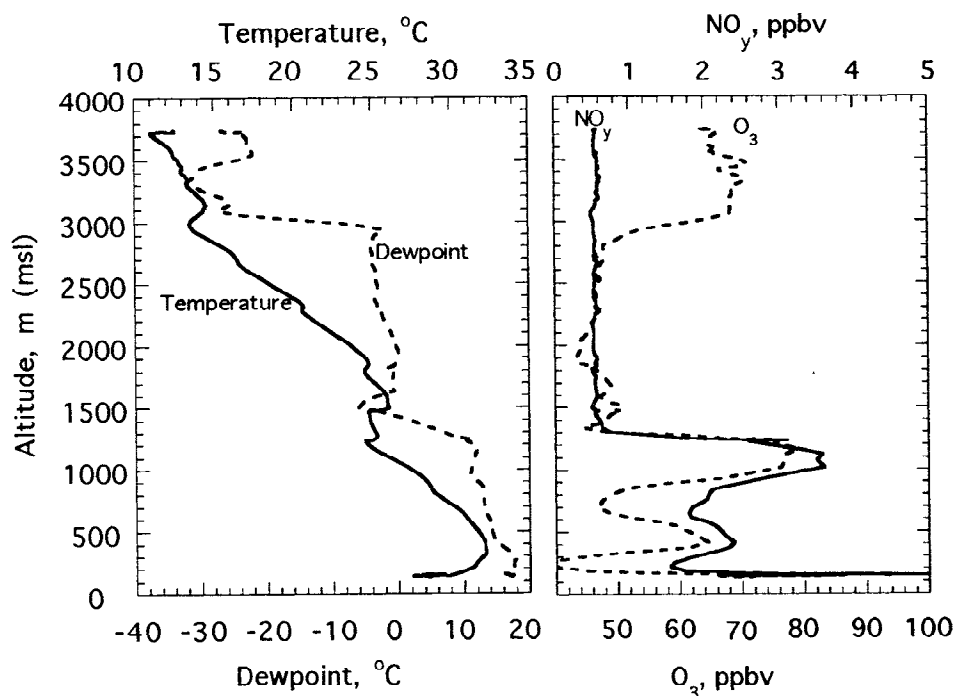


Figure 3. Flight tracks corresponding to plumes sampled on August 27, and August 28, 1993. Solid lines with arrows superimposed are back trajectories from the indicated locations. Arrows are plotted every 6 hours.



**Figure 4.** Atmospheric sounding made by the G-1 at approximately 42.1°N, 69°W at midday on August 27, 1993. a, temperature and dew point, b, O<sub>3</sub> and NO<sub>y</sub>.

maximum values that are appreciable in the context of the location at which the measurements were made. O<sub>3</sub> peaked at 110 ppbv, Figure 5a, and corresponded to peak concentrations of CO of 380 ppbv, NO<sub>y</sub> of 17 ppbv, and accumulation mode aerosol number densities of 2500/cm<sup>3</sup>. As the flight track approached the southern tip of Nova Scotia, concentrations fell to 20–50% of their peak values.

A filter sample collected in the portion of the flight indicated in Figure 5, exhibited an aerosol-S concentration of 1.9 ppbv, an SO<sub>2</sub> concentration of 4.5 ppbv, and an HNO<sub>3</sub> concentration of 6 ppbv. The high HNO<sub>3</sub> is consistent with the NO<sub>y</sub> and NO<sub>x</sub> measurements (Figure 5b), indicating that a substantial amount of the NO<sub>x</sub> initially present in this air mass had been converted to NO<sub>x</sub> oxidation products by the time these measurements were made. Low NO<sub>x</sub>/NO<sub>y</sub> ratios were characteristic of most of the data reported here. The apparent anticorrelation of the H<sub>2</sub>O<sub>2</sub> concentration (Figure 5c) with the concentrations of other trace species (particularly NO<sub>x</sub>), is consistent with our perception that the formation rate of peroxide is slow until NO<sub>x</sub> concentrations have been reduced to very low values. At NO<sub>x</sub> concentrations corresponding to the peak values shown in Figure 5, most radicals will be removed from the system by formation of HNO<sub>3</sub> rather than combine to form peroxides. Peroxide formation rates will be larger at NO<sub>x</sub> concentrations corresponding to those on the right side of Figure 5.

Meteorological and trace gas data corresponding to the flight made on August 28, 1993, is shown in Figures 6 and 7. Figure 6 shows a sounding conducted at the southern extremity of the August 28 flight track (Figure 3). This location is approximately 800 km downwind of major source regions in the northeastern United States. The temperature sounding indicates a stable atmosphere with strong inversions at ~500 m and at ~1700 m. The dew point sounding shows a moist layer near the ocean surface, and a layer of uniform humidity between the 500- and 1700-m inversions; above 1700 m, the air is considerably drier and the dew point is more variable. Back trajectories calculated

for end points at altitudes of 200, 800, and 1000 m indicate that the air in the moist layer between 500 and 1400 m had been over the heavily industrialized northeast corridor of the United States between the cities of New York and Boston about 48 hours previous. This transport time is considerably longer than for the plume sampled on August 27, 1993. The back trajectory with an ending altitude of 800 m is shown in Figure 3.

Vertical profiles of selected chemical species measured during the August 28 sounding are given in Figure 6. Note that while most of the pollutants are trapped in the region between the two strong inversions at 500 and 1500 m, relatively polluted air is also present below the lowest inversion topping at ~500 m. Qualitatively, the vertical structure of the trace gas concentrations displayed in Figure 6 is highly coherent with O<sub>3</sub>, CO, NO<sub>y</sub>, and H<sub>2</sub>O<sub>2</sub> all exhibiting maximum concentrations in a layer, approximately 1 km thick, trapped between the 500- and 1500-m inversions. An interesting feature of the profile is the covariance of the hydrogen peroxide concentration with concentrations of the other trace species. This covariance, in combination with the very high peroxide concentrations, may be taken as an indication that the air mass is well aged in a photochemical sense.

Concentrations of trace species and the location of the filter sample measured during a long transect between 42°N latitude and 44°N latitude on the 62°W longitude line are shown in Figure 7. The altitude of this transect (600 m) is between the two strong temperature inversions shown in Figure 6. Concentrations are plotted as a function of latitude along the flight track for August 28, 1993, indicated in Figure 3. Peak concentrations of various trace species observed during this long transect were the highest measured during the entire program. The maximum O<sub>3</sub> concentration was nearly 150 ppbv, and was associated with a CO concentration of ~480 ppbv, an NO<sub>y</sub> concentration of 18 ppbv, and an accumulation mode particle number density of 2500 cm<sup>-3</sup>. A filter sample collected at the center of the plume, as indicated in Figure 7, exhibited an

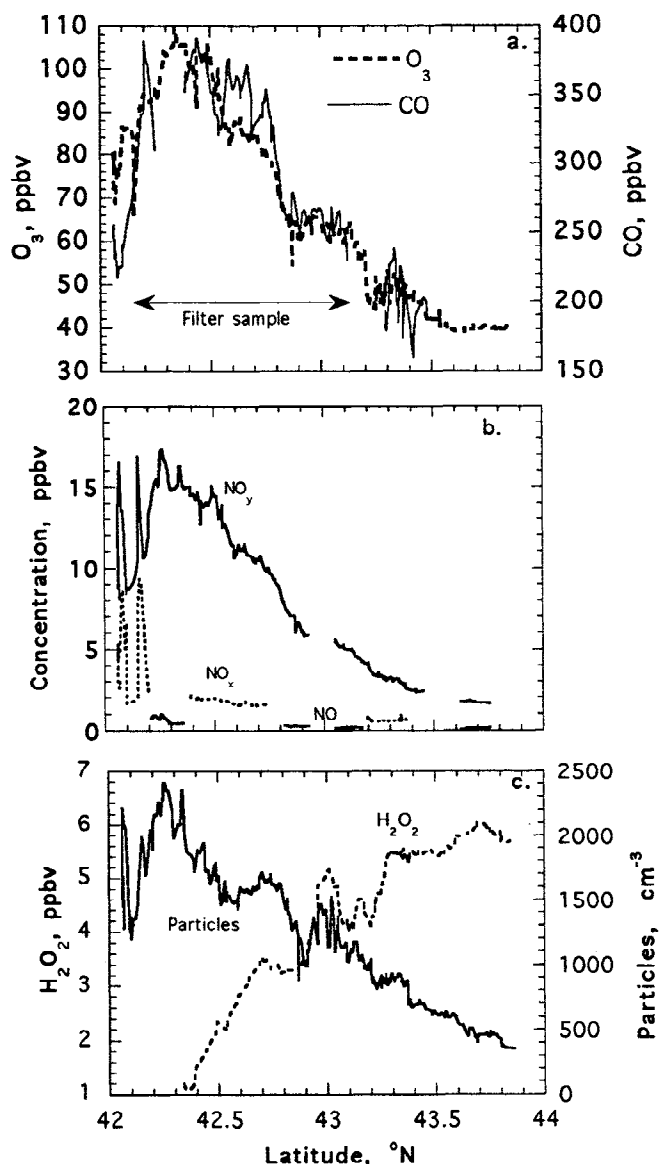


**Figure 5.** Concentrations of CO and O<sub>3</sub> (a), NO<sub>y</sub>, NO<sub>x</sub>, and NO (b), particles and H<sub>2</sub>O<sub>2</sub> (c) measured at an altitude of 140 m, mean sea level on a flight from 42°N, 69°W toward Chebogue Point, Nova Scotia on August 27, 1993.

aerosol-S concentration of 4.2 ppbv, an SO<sub>2</sub> concentration of 4.3 ppbv and an HNO<sub>3</sub> concentration of 11.4 ppbv. Back trajectory analysis indicated that the air mass had last been over coastal source regions 2 to 3 days prior to the measurements. This long residence time is consistent with the extensive photochemical processing necessary to produce the high O<sub>3</sub> concentrations and photochemical product species that were observed.

Figure 7 also emphasizes the widespread geographical extent of these plumes, with O<sub>3</sub> concentrations in excess of 90 ppbv extending over a distance of at least 250 km. Measurements from other NARE aircraft flying at this time suggest that the export of pollutants from the northeastern United States to the North Atlantic was even more widespread than indicated by data shown here. Twin Otter flights in the vicinity of Chebogue Point at the southern tip of Nova Scotia observed high concentrations of O<sub>3</sub> and related species; similar observations were made during an extensive flight of the King Air aircraft from Portland, Maine, to Sable Island.

Several features of the data shown for the flights of August 27 and 28 should be emphasized since they are common to most of the North Atlantic plume data that we have examined. One feature is that the plumes are transported in well-defined layers bounded by strong inversions. In combination with the presence of a stable to neutral lapse rate (which was always observed), these inversions will limit mixing of the pollutants trapped in these layers with the surrounding atmosphere, or down to the ocean surface. The presence and apparent persistence of these layers is no doubt due to transport over the cold North Atlantic which causes the formation of a strong inversion near the ocean surface and stabilizes the atmosphere. This lack of vertical mixing is in distinct contrast to the situation over the continent where solar heating during the day promotes the formation of a well-mixed boundary layer. This causes the trace gases to be much more homogeneously mixed throughout the lower portion of the troposphere. Such mixing also maximizes losses of species to the surface by dry deposition. The presence of pollutants as stable layers as observed here promotes retention of product species and minimizes losses of pollutants to the surface.

### 3.2. Plume Composition

As suggested by Figures 4 through 7, plume composition was characterized by high concentrations of O<sub>3</sub>, NO<sub>x</sub> oxidation products, and aerosol particles, similar in many respects to what might be observed in a photochemically well-aged urban air mass over the North American continent [Daum et al., 1989; Trainer et al., 1991; Doddridge et al., 1992; Olszyna et al., 1994; Kleinman et al., 1994]. Table 3 gives the median, maximum, and standard deviation of the concentrations of selected species measured in all of the plumes sampled during our flights. For comparison, statistics on concentrations measured under background conditions are also given. For present purposes, background concentrations were defined as measurements made when back trajectories indicated transport from nonsource regions, principally from the northwest, east, and northeast. Further, we considered only measurements made in the lowest 2 km of the atmosphere, the altitude range (Figure 2) in which the transported plumes were sampled. Background data included flights made on August 16, 17, 18, and 22. With the exception of the flight on August 16, all background flights included measurements in the vicinity of Sable Island.

Obviously, plume concentrations of these species were much higher than concentrations measured in background air, particularly species such as HNO<sub>3</sub> and aerosol-S, where plume concentrations exceeded background concentrations by more than a factor of 10. This is not unexpected because these species are rapidly formed in the atmosphere and have relatively short residence times. For species with significantly longer residence times or having significant background concentrations, such as CO or O<sub>3</sub>, differences between plume and background concentrations were on the order of a factor of 2, or less.

**Ozone and peroxides.** Mean and maximum O<sub>3</sub> concentration (Table 3) were within the range of values observed in plumes advected off the east coast of the United States during summer in other programs [e.g., Anderson et al., 1993; Parrish et al., 1993a]. They were also similar to values found in summertime surface measurements at various locations in the northeastern United States [e.g., Kleinman et al., 1994; Trainer et al., 1991; Olszyna et al., 1994]. Peroxide concentrations were quite high (Table 3), reaching a maximum concentration of 11 ppbv on a flight on August 28, 1993, in a photochemically well aged air mass 3 to 4 days downwind of source regions.

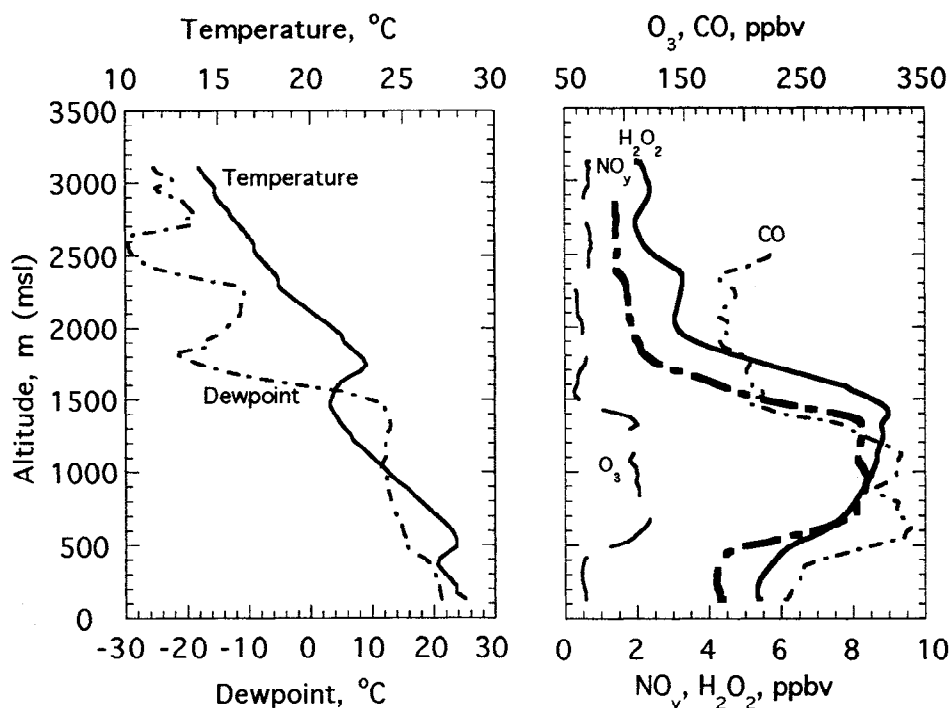


Figure 6. Atmospheric sounding made by the G-1 at approximately 42°N, 62°W at midday on August 28, 1993.

There are few equivalent measurements to which these peroxide concentrations may be compared. Airborne measurements made in the boundary layer in the summer [e.g., Heikes *et al.*, 1987; Daum *et al.*, 1990; Boatman *et al.*, 1989], all indicate concentrations somewhat lower than measured here. However,

since we have chosen to consider here only data in photochemically well-aged plumes, whereas previous reports of airborne studies did not segregate their data in this way, this difference may not be significant. Surface measurements made in the eastern United States during summer are considerably lower than measured here [e.g., Lee *et al.*, 1993]. The latter is probably due to the importance of dry deposition of peroxides in surface measurements, and to the constant admixture of  $\text{NO}_x$  to the air near the surface, which suppresses peroxide formation.

Peroxide concentrations were correlated with  $\text{O}_3$  ( $r^2 = 0.47$ ) and with the product of the ozone and water vapor mixing ratios ( $r^2 = 0.49$ ). A reasonable degree of correlation between these quantities is expected since the principal source of radicals for peroxide formation is ozone photolysis to form excited state oxygen,  $\text{O}(^1D)$ , followed by reaction of  $\text{O}(^1D)$  with water vapor to form OH. That the correlation of peroxide with  $\text{O}_3 \cdot \text{H}_2\text{O}$  is only nominally better than with  $\text{O}_3$  alone probably arises from the relatively small range of water vapor concentrations encountered during these measurements.

The correlation of peroxide with both  $\text{O}_3$  and  $\text{O}_3 \cdot \text{H}_2\text{O}$  is consistent with our perception that the sampled air masses were well aged in a photochemical sense. In air masses that have only recently been mixed with fresh emissions,  $\text{NO}_x$  concentrations will be high and radicals generated by  $\text{O}_3$  photolysis will be removed principally by reaction with  $\text{NO}_2$  to form  $\text{HNO}_3$ . It is only under low the  $\text{NO}_x$  conditions characteristic of aged air masses that radical/radical combination reactions producing peroxides become important. A more comprehensive analysis of peroxide concentrations, and their relationship to the concentrations of other atmospheric trace species is in preparation [J. Weinstein-Lloyd *et al.*, this issue].

**$\text{NO}_y$  concentrations and speciation.** Prior to discussing  $\text{NO}_y$  concentrations and speciation, it is important to review the limitations of the  $\text{NO}_y$  instrument that was used to make these measurements. This instrument had two channels; one channel was always used to measure  $\text{NO}_y$ , the other channel was switched between measuring NO and  $\text{NO}_x$ , with  $\text{NO}_x$  measurements being emphasized (NO was measured about one third of

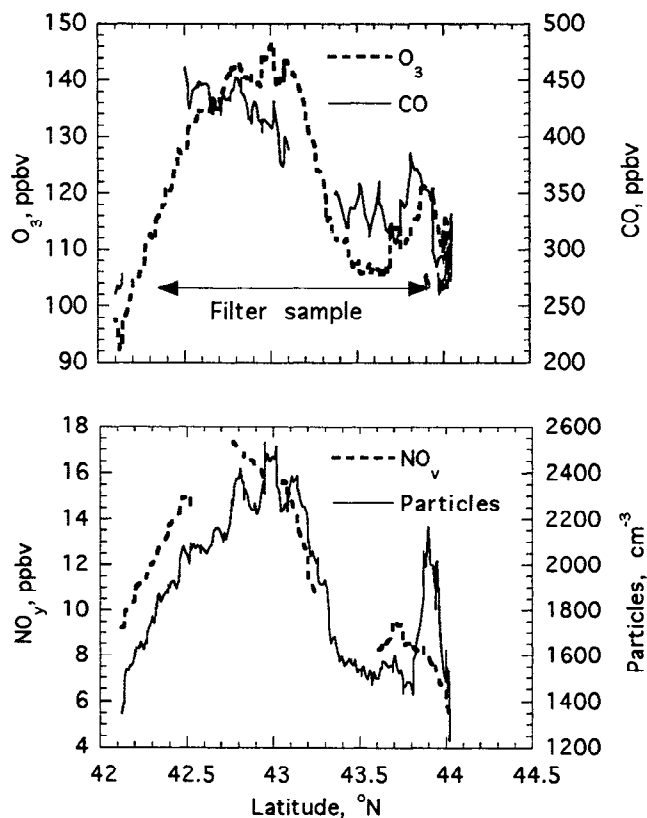


Figure 7. Trace gas and aerosol concentrations measured at an altitude of 600 m, mean sea level on a flight from 42°N to 44°N on the 62°W latitude line.



Table 3. Comparison of Plume and Background Concentrations

Species	Background Median/Plume Median	Background $\sigma^c$ /Plume $\sigma$	Background Maximum/Plume Maximum
O <sub>3</sub>	31/56	7.4/22	55/147
NO <sub>y</sub>	0.44/2.1	0.28/3.1	3.6/17.4
HNO <sub>3</sub> <sup>a</sup>	0.10/2.6		0.2/11.4
Aerosol S <sup>a</sup>	0.34/1.5		0.38/5.0
CO	148/205	48/68	284/452
SO <sub>2</sub> <sup>a</sup>	0.06/1.35	0.06/0.6	0.3/4.5
H <sub>2</sub> O <sub>2</sub>	2.1/3.6	1.1/2.5	5.3/11.0
Particle number density <sup>b</sup>	208/574	491/528	620/2728

<sup>a</sup> Measured by filter collection and analysis<sup>b</sup> 0.2 < d < 3  $\mu$ m<sup>c</sup>  $\sigma$  = standard deviation

the time and NO<sub>x</sub> about two thirds of the time). Thus there are no simultaneous measurements of NO and NO<sub>x</sub> from which photostationary state evaluations can be made. It is also important to recognize that the estimated uncertainty in the NO channel was of the order of 30 to 40 ppt, causing significant uncertainty in the mean values of NO, and that the "NO<sub>x</sub>" may have a positive bias of as much as 20% because the data could not reliably be corrected for the NO concentration (see section 2).

The median and mean concentrations NO, NO<sub>x</sub>, NO<sub>y</sub> and the ratios of NO<sub>x</sub>/NO<sub>y</sub>, and NO/NO<sub>y</sub> concentrations are given in Table 4. Since the NO, NO<sub>x</sub>, and HNO<sub>3</sub> measurements were not made simultaneously, Table 4 also includes the median O<sub>3</sub> and NO<sub>y</sub> concentrations during the time when each of these species were measured to establish whether the range of conditions was similar. It is evident that there are small differences in the NO<sub>y</sub> and O<sub>3</sub> concentrations when the various species were measured, and this will introduce some uncertainty in our subsequent discussion of the distribution of NO<sub>y</sub> into its various components.

The median ratio of NO<sub>x</sub>/NO<sub>y</sub> of 0.16 suggests that only small fraction of NO<sub>y</sub> was present as NO<sub>x</sub>; we consider this number as an upper bound due to the bias in our NO<sub>x</sub> measurements. This low NO<sub>x</sub> fraction is consistent with the high t-NO<sub>3</sub><sup>-</sup> concentrations (t-NO<sub>3</sub><sup>-</sup> (max) = 12 ppbv) that were observed, and with the very high fraction (mean ~72%) of total NO<sub>y</sub> that these concentrations represent. The vast majority of t-NO<sub>3</sub><sup>-</sup> was measured as HNO<sub>3</sub> (median value 70%). Regression of the t-NO<sub>3</sub><sup>-</sup> against the NO<sub>y</sub> concentration exhibited a slope of 0.8, an intercept of -0.05, and an  $r^2$  = 0.9. The high degree of correlation suggests that the presence of high fractional t-NO<sub>3</sub><sup>-</sup> is a general feature of the plumes sampled during this set of flights. The low NO<sub>x</sub> and high t-NO<sub>3</sub><sup>-</sup> is also consistent with our

conjecture (unfortunately not measured) that the concentration of peroxyacetyl nitrate, the other major NO<sub>x</sub> oxidation product, would be low under the conditions of the measurements, that is, relatively high temperatures and relatively low concentrations of NO<sub>x</sub>.

Comparison of both NO<sub>y</sub> concentrations and speciation to previous measurements in photochemically aged air masses reveals some interesting similarities and differences. In surface measurements made at six rural sites in the eastern United States during late summer and early fall, Parrish *et al.* [1993b], observed NO<sub>y</sub> concentrations between ~1 and 30 ppbv, with median concentrations of 2-5 ppbv, comparable to the range of concentrations reported here. The median daytime NO<sub>x</sub>/NO<sub>y</sub> concentration ratios of 0.25-0.4, are considerably higher than found over the WNAO. Doddridge *et al.* [1992], found the median concentration of NO<sub>y</sub> at a rural site in Virginia to be 3.5 ppbv, and the median NO/NO<sub>y</sub> ratio to be ~0.038 (NO<sub>2</sub> was not measured). Doddridge also found that approximately 39% of NO<sub>y</sub> was present as nitrate which is substantial, but not nearly so high as found during NARE. Buhr *et al.* [1990] found that HNO<sub>3</sub> represented about 45% of the NO<sub>y</sub>, and PAN about 20% in air masses that had been highly processed photochemically (i.e., NO<sub>x</sub>/NO<sub>y</sub> < 0.2). Buhr also observed that as the NO<sub>x</sub>/NO<sub>y</sub> ratio decreased, the fraction of NO<sub>y</sub> present as HNO<sub>3</sub> increased, while the fraction present as PAN decreased. This was attributed to high temperatures, humidity, and solar UV radiation prevailing during the sampling of highly processed air masses. Such conditions promote the loss of thermally labile PAN and also contribute to the more rapid formation of HNO<sub>3</sub> due to the high production rate of OH. In a surface-based study conducted in Metter, Georgia, during the summer of 1992 during midday (1000-1400 EST), the NO<sub>x</sub>/NO<sub>y</sub> ratio was ~0.3, total-nitrate/NO<sub>y</sub> was ~0.45, and the PAN/NO<sub>y</sub> was ~0.13 [Kleinman, 1994].

It is interesting to speculate on the reasons why the t-NO<sub>3</sub><sup>-</sup>/NO<sub>y</sub> ratio is so much larger in pollutant plumes advected out over the North Atlantic than in surface measurements made in photochemically aged air masses in the eastern United States. An important consideration may be that most of our measurements were made in isolated layers of pollutants encountered from 1 to 5 days downwind of east coast source regions. Thus, all of the samples were collected in air masses that were well aged photochemically as indicated by the low ratios of NO<sub>x</sub>/NO<sub>y</sub> and high concentrations of O<sub>3</sub>. As noted above such aged air masses are expected to have relatively high t-NO<sub>3</sub><sup>-</sup>/NO<sub>y</sub> ratios because HNO<sub>3</sub> is the end product of NO<sub>x</sub> oxidation, and because PAN, which may have been formed during the initial stages of photochemical aging will decompose to NO<sub>x</sub> and be converted to HNO<sub>3</sub> under conditions prevailing in our measurements (i.e.,

Table 4. NO<sub>y</sub> Speciation

Quantity	Mean/Median	Median O <sub>3</sub> /Median NO <sub>y</sub>
NO <sub>y</sub> (ppbv)	3.31/2.1	56/2.1
NO <sub>x</sub> (ppbv)	0.46/0.36	58/2.0
NO (ppbv)	0.15/0.12	61/2.8
NO <sub>x</sub> /NO <sub>y</sub>	0.19/0.16	--
NO/NO <sub>y</sub>	0.05/0.04	--
t-NO <sub>3</sub> <sup>a</sup> /NO <sub>y</sub>	0.72/0.71	59/2.9

<sup>a</sup> Measurements of t-NO<sub>3</sub><sup>-</sup> were made by analysis of filter samples which were collected for periods of 15-60 min, depending on conditions; t-NO<sub>3</sub><sup>-</sup> is defined as the sum of aerosol and HNO<sub>3</sub> nitrate. The ratio was computed from the measured t-NO<sub>3</sub><sup>-</sup> and the average NO<sub>y</sub> measured during the filter collection period.

**Table 5.** Aerosol Composition

Quantity	Mean	Median	Standard Deviation
NH <sub>4</sub> <sup>+</sup> (ppbv)	1.8	1.3	1.4
Na <sup>+</sup> (ppbv)	0.3	0.2	0.3
NO <sub>3</sub> <sup>-</sup> (ppbv)	0.5	0.5	0.2
SO <sub>4</sub> <sup>=</sup> (ppbv)	1.7	1.4	1.5
Cl <sup>-</sup> (ppbv)	0.1	0.01	0.35
NO <sub>3</sub> <sup>-</sup> /SO <sub>4</sub> <sup>=</sup>	0.54	0.3	0.3
NH <sub>4</sub> <sup>+</sup> /SO <sub>4</sub> <sup>=</sup>	1.2	1.2	0.4

relatively high temperatures, clear skies, and high moisture content). Equally important is that losses of HNO<sub>3</sub> by dry deposition would be minimal under the conditions under which these measurements were made (i.e., pollutants were present in stable layers transported over a cold ocean surface, leading to low deposition velocities). In contrast, concentrations of HNO<sub>3</sub> measured at continental surface sites are strongly influenced by the effects of dry deposition because of surface heating and consequent mixing of the boundary layer. For the measurements reported here, NO<sub>y</sub> was usually found in layers well removed from the surface and almost always isolated from it by a low-level inversion. Thus the high t-NO<sub>3</sub>/NO<sub>y</sub> ratios observed are not unreasonable in the context of the conditions under which the measurements were made.

**Aerosol composition.** At least one filter sample was collected during each of the flights to measure aerosol mass and composition. Average concentrations of aerosol species and relevant statistics are given in Table 5. Such concentrations are typical of those that would be measured in a moderately polluted air mass over the northeastern United States. The highest aerosol mass concentration (4.2 ppbv sulfate and 0.2 ppbv nitrate) was measured in the plume sampled on August 28, 1993, (sampling location indicated in Figure 7). As expected the composition of the aerosol samples was dominated by sulfates. The average nitrate to sulfate molar ratio was 0.54, and the sulfate concentration was well correlated ( $r^2 = 0.64$ ,  $n = 11$ ) with the accumulation aerosol number density measured by the ASASP probe. Aerosol nitrate represented only a small fraction of the total nitrate present; the average ratio of aerosol nitrate to the sum of aerosol nitrate and nitric acid was 0.28. Aerosol chloride was quite small, probably due to a reaction of aerosol chloride with the high concentrations of nitric acid in the atmosphere releasing HCl which was not collected on the aerosol filter. Although aerosol acidity was not directly measured, the average NH<sub>4</sub><sup>+</sup>/SO<sub>4</sub><sup>=</sup> molar ratio of 1.2 suggests that on average, the aerosol was nearly as acidic as ammonium bisulfate. The generally low concentrations of Na<sup>+</sup> (average, 0.3 ppbv) indicate the presence of only nominal amounts of sea salt. The latter is consistent with the plumes being generally located in isolated layers well above the surface.

### 3.3. Relationships Between Plume Constituents

Here we examine the relationship between concentrations of various trace gases and compare these relationships to those measured under other conditions and in other programs both as a means of understanding the current data and establishing their representativeness.

**Correlations with CO.** CO is a long-lived tracer of anthropogenic pollution. Its principal source is combustion of fossil fuel, and to a lesser extent, the atmospheric oxidation of hydrocarbons. CO has been found to be an effective means of

distinguishing between natural and anthropogenic sources of O<sub>3</sub> and other trace species. A fairly consistent relationship between CO and O<sub>3</sub> has been observed in measurements in the eastern United States and over the WNAO. For measurements made in the summer at surface sites in the eastern US in photochemically aged air masses, CO and O<sub>3</sub> are generally found to be well correlated ( $r^2 > 0.5$ ) with regression slopes tightly grouped about 0.3 [Chin *et al.*, 1994, and references therein]. Similar results were obtained from analysis of measurements made in the western North Atlantic in the NARE operational region during the summer of 1991 [Parrish *et al.*, 1993a], where regression slopes ranged between 0.21 and 0.30 for sites at several distances downwind from east coast source regions. A somewhat higher slope (0.41) was observed in aircraft measurements made over the western North Atlantic east of the mid-Atlantic states during the Global Transport Experiment/Chemical Instrumentation Test and Evaluation (GTE/CITE 3) program in the summer of 1989 [Anderson *et al.*, 1993]. Observations from the Arctic Boundary Layer Expedition (ABLE 3b) exhibit slopes in the range 0.2-0.69 for anthropogenic pollutant plumes sampled in the free troposphere over eastern Canada [Mauzerall, *et al.*, 1993]. The results of these experimental studies were quite similar to both the modeled distributions of CO and O<sub>3</sub> concentrations and to the statistical relationship between these two species. The analysis of Chin *et al.* [1994] concludes that an O<sub>3</sub>/CO slope of ~0.3 is a common characteristic of boundary layer air over eastern North America in the summer.

Because of the interest in CO/O<sub>3</sub> relationships as a means of evaluating photochemical models and for estimating the amount of O<sub>3</sub> exported to the surrounding atmosphere by the United States during summer, this relationship is also examined here. It may be argued that current measurements are unique in the sense that they were made aloft in isolated, well-aged plumes of photochemical pollutants that have been transported significant distances from source regions, and would thus provide an important set of data with which to examine the generality of previous modeling and experimental studies. Shown in Figure 8

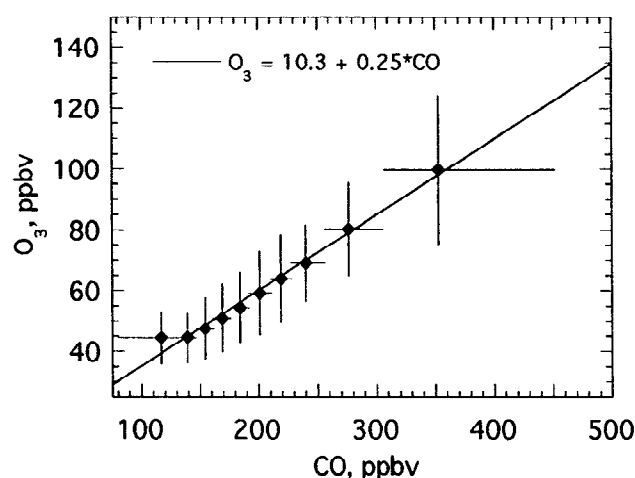


**Figure 8.** Binned O<sub>3</sub> concentration as a function of the binned CO concentration. One-minute averaged data were ordered by CO concentration and divided into 10 intervals. Each point on the plot represents the average CO and O<sub>3</sub> in the interval. Horizontal bars represent the range of CO concentration included in each of the points; vertical bars represent the standard deviation of the O<sub>3</sub> concentration over the indicated range of CO concentrations. Slope and intercept were calculated from the individual data points.

is a plot of all of the concurrent CO and O<sub>3</sub> plume data measured during the program. For clarity in presentation we have ordered the data by CO concentration into 10 bins, each representing 10% of the data. With the exception of the bin at the lowest CO concentration, O<sub>3</sub> increases linearly with CO over a wide range of CO concentrations. The slope and correlation coefficient for the unbinned data are 0.26 and 0.8, respectively; the intercept is of the order of 10 ppbv. Both the slope and correlation coefficient for the plume data are well within the range of these quantities that have been reported elsewhere, and in particular agree quite well with surface measurements made in the NARE operational region during July and August 1991 [Parrish *et al.*, 1993a]. This agreement gives further support to estimates of the amount of O<sub>3</sub> exported from the United States to the North Atlantic as reported by Parrish *et al.* [1993a] and Chin *et al.* [1994].

It is of additional interest to explore the relationship between CO and other species that may be of anthropogenic origin, namely, NO<sub>y</sub> and accumulation mode aerosol particle number density, N<sub>ap</sub>. Both of these species are as well correlated with CO as is O<sub>3</sub>. The correlation coefficient between NO<sub>y</sub> and CO is 0.82 and the slope is 0.038 ppbv NO<sub>y</sub>/ppbv CO. For aerosol number density the correlation coefficient with CO is 0.80, and the slope is 6.2 cm<sup>-3</sup>/ppbv. The slope and correlation coefficient between CO and N<sub>ap</sub> are similar to values (0.88 and 7.7 cm<sup>-3</sup>/ppbv) reported by Anderson *et al.* [1993] in measurements made in continental plumes transported over the North Atlantic Ocean in late summer 1989.

The high degree of correlation between CO and NO<sub>y</sub>, and between CO and N<sub>ap</sub> is consistent with a common source for these species. However, it is somewhat surprising that these correlations are as good as between O<sub>3</sub> and CO. In particular, the good correlation between CO and NO<sub>y</sub> is unexpected because most of the NO<sub>y</sub> is present as HNO<sub>3</sub> which is readily lost from the atmosphere by deposition. Similar arguments apply to accumulation mode aerosol particles which may be readily lost by wet deposition. The high degree of correlation that was observed reinforces the view that these species had been transported under conditions such that their losses were minimized (i.e., under nonprecipitating conditions in elevated plumes that were not in contact with the surface).

**Correlation of NO<sub>y</sub> and NO<sub>x</sub> with O<sub>3</sub>.** The relationship between O<sub>3</sub> and NO<sub>y</sub> concentrations, and between O<sub>3</sub> and the concentrations of the products of NO<sub>x</sub> oxidation (i.e., HNO<sub>3</sub>, peroxyacetyl nitrate, and other organic nitrates), NO<sub>z</sub> (NO<sub>z</sub> = NO<sub>y</sub> - NO<sub>x</sub>), has been the subject of considerable recent study [e.g., Trainer *et al.*, 1993; Olszyna *et al.*, 1994]. The motivation for such study has been to evaluate the response of O<sub>3</sub> concentrations to changes in NO<sub>x</sub> emissions. Knowledge of the production efficiency and the NO<sub>x</sub> source strength allows an estimate of the total amount of ozone formed. O<sub>3</sub> and NO<sub>x</sub> are linked because the only photochemical reaction that is known to produce O<sub>3</sub> in the troposphere is the reaction of peroxy radicals with NO, producing NO<sub>2</sub> which is subsequently photolyzed in the presence of O<sub>2</sub> to produce NO and O<sub>3</sub>.

Modeling studies predict that the amount of O<sub>3</sub> produced per NO<sub>x</sub> oxidized will depend nonlinearly on the NO<sub>x</sub> concentration, with ozone production efficiency decreasing with increasing NO<sub>x</sub> concentrations [Liu *et al.*, 1987; Lin *et al.* 1988]. In regions far from NO<sub>x</sub> sources, it is thought that the production of O<sub>3</sub> is NO<sub>x</sub> limited. The relationship between O<sub>3</sub> and NO<sub>y</sub>, and between O<sub>3</sub> and NO<sub>x</sub> oxidation products has been examined most frequently for data collected at the surface. To our knowledge, it has not been studied in aged, polluted air masses that have been isolated from hydrocarbon and NO<sub>x</sub> sources for periods of several days and in an environment where losses of

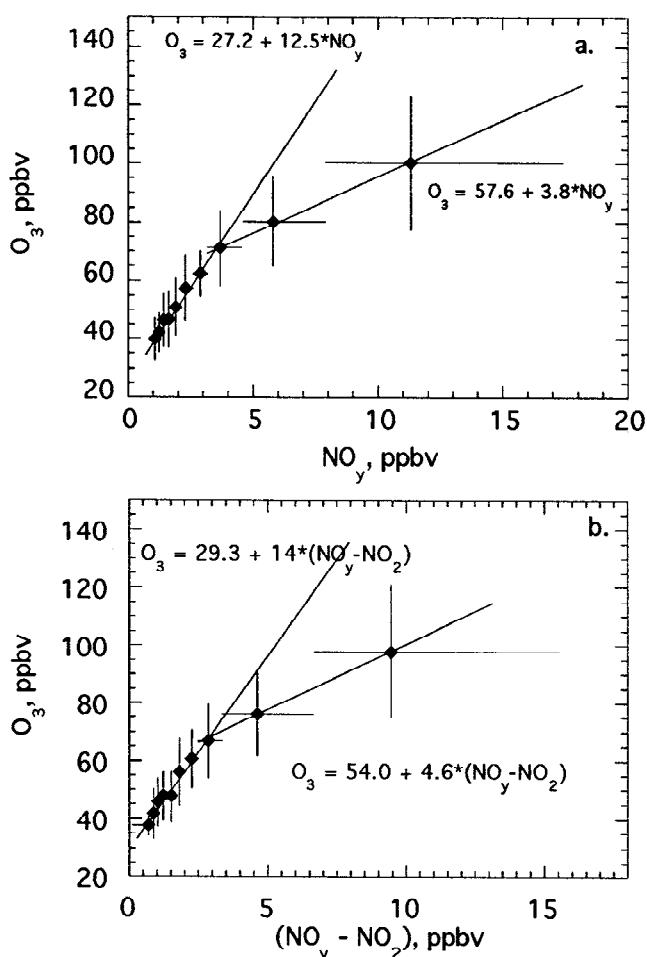


**Figure 9.** Binned O<sub>3</sub> concentration as a function of the binned (a) NO<sub>y</sub> and (b) (NO<sub>y</sub> - NO<sub>x</sub>) concentration. Ten-second data were ordered by NO<sub>y</sub> or (NO<sub>y</sub> - NO<sub>x</sub>) concentration and divided into 10 intervals. Each point on the plot represents the average NO<sub>y</sub> or (NO<sub>y</sub> - NO<sub>x</sub>), and average O<sub>3</sub> for the interval. Horizontal bars represent the concentration range for the interval; vertical bars represent the standard deviation of the O<sub>3</sub> concentration for the interval. Slope and intercept were calculated from the individual data points.

photochemical reaction products to the surface by either dry or wet deposition was minimized.

In the following analysis we examine both the relationship between O<sub>3</sub> and NO<sub>y</sub>, and between O<sub>3</sub> and NO<sub>z</sub>. In the latter analysis we acknowledge a positive bias in our estimates of NO<sub>x</sub>, but since NO<sub>x</sub> is generally such a small fraction of NO<sub>y</sub>, this does not significantly influence our analysis. Figure 9a shows a plot of the O<sub>3</sub> concentration as a function of the NO<sub>y</sub> concentration in which the data have been divided into 10 bins each containing 10% of the data. Figure 9a exhibits some interesting features. Clearly the data can be divided into low and high NO<sub>y</sub> groups corresponding to NO<sub>y</sub> concentrations approximately < 3 ppbv, and greater than 5 ppbv. The slope of the low concentration group is 12.5 ppbv O<sub>3</sub>/ppbv NO<sub>y</sub>; the slope of the high concentration group is only 3.8 ppbv O<sub>3</sub>/ppbv NO<sub>y</sub> (slopes for the two regions were calculated from the individual data points). Figure 9b shows the corresponding plot of O<sub>3</sub> vs. NO<sub>z</sub>. The latter plot exhibits a slope of 14 ppbv O<sub>3</sub>/ppbv NO<sub>z</sub> in the low concentration region and a slope of 4.6 ppbv O<sub>3</sub>/ppbv NO<sub>z</sub> in the high concentration region; these are very similar to the slopes calculated from the O<sub>3</sub>-NO<sub>y</sub> data. The latter is expected

considering that for the vast majority of these measurements most of the  $\text{NO}_y$  (> 85%) had been converted to  $\text{HNO}_3$ , PAN, and other  $\text{NO}_x$  oxidation products. It is interesting that almost all of the data included in the high  $\text{NO}_y$  regime ( $\text{NO}_y > 3$  ppbv) came from flights made on August 27 and 28, in transported plumes that were well defined spatially. Data in the low-concentration regime were generally collected under less well-defined conditions. Radon measurements corresponding to high  $\text{NO}_y$  concentrations exhibited higher radon concentrations than the measurements that were associated with the low  $\text{NO}_y$  measurements [Zaucker *et al.*, this issue].

The slope of  $\text{NO}_z$  versus  $\text{O}_3$  at low concentrations is within the range of values that have been reported by others. In an analysis of the midday  $\text{NO}_y/\text{O}_3$  data collected more or less concurrently at six sites in the eastern United States and Canada, the relationships between  $\text{O}_3$  and  $\text{NO}_z$  were found to be quite similar. At Scotia, Pennsylvania, it was observed that ozone concentrations could be well approximated by a straight line with a slope of 8.5 ppbv  $\text{O}_3$ /ppbv  $\text{NO}_z$  up to  $\text{NO}_z$  concentrations of 10 ppbv [Trainer *et al.*, 1993]. In data taken during the same program at Egbert, Ontario, a similar slope up to an ( $\text{NO}_y - \text{NO}_x$ ) concentration of about 5 ppbv was observed. At higher concentrations, the slope decreased considerably, a point which will be discussed below. Olszyna *et al.* [1994], found a slope of 12.3 for  $\text{NO}_z$  concentrations ranging between 0.5 and 5 ppbv in measurements made during a 6-week period in the summer of 1991 in central Tennessee. Kleinman *et al.* [1994] found the slope of  $\text{O}_3$  vs.  $\text{NO}_2$  to be 11.4, with an intercept of 27 and an  $r^2$  value of 0.78 for hourly averaged data in summertime measurements in Metter, Georgia; the corresponding slope and intercept for  $\text{O}_3$  versus  $\text{NO}_y$  was 10.3 with an  $r^2$  value of 0.72. In part, differences in  $\text{O}_3$ - $\text{NO}_y$  dependencies between various programs have been attributed to differences in the concentrations and consequent influence of biogenic hydrocarbons which, in combination with  $\text{NO}_x$  concentrations, are known to influence  $\text{O}_3$  production. This same reasoning may apply to differences between measurements made aloft over the North Atlantic and previous measurements cited above, but other factors may be important as well.

The much lower slope (3.8) of the  $\text{O}_3$  versus  $\text{NO}_z$  plot of our data at high concentrations of  $\text{NO}_z$  in comparison both to the value calculated at low concentrations, and to the values calculated for other data sets is interesting. The slope is similar to the value of 3.6 we calculate from the Egbert, Ontario, data as displayed in Figure 4 of Trainer, *et al.* (1993), over the concentration range ~5–20 ppbv. It is also similar to modeled values of  $\text{O}_3$  vs.  $\text{NO}_z$ , as discussed in Trainer *et al.* [1993], which exhibit a decreasing slope with increasing  $\text{NO}_z$  concentration; below  $\text{NO}_z$  concentrations of about 4 ppbv the slope is ~13; in the concentration range 5–10 ppbv, the slope is ~4. The slopes from both the low- and high-concentration ranges match the slopes derived from the NARE data very closely; whether this agreement is fortuitous or due to underlying chemical/physical processes will be discussed below. The variation of the  $\text{O}_3/\text{NO}_z$  slope as a function of  $\text{NO}_z$  concentration is also consistent with calculations [Liu *et al.*, 1987] suggesting that the efficiency of  $\text{O}_3$  production per unit  $\text{NO}_x$  increases with decreasing  $\text{NO}_x$  concentration.

It is interesting to speculate as to whether the curvature observed in our data at high  $\text{NO}_y$  concentrations reflects a variation in  $\text{O}_3$  production efficiency with  $\text{NO}_x$  concentration as predicted by models, or whether it may be due to other factors. One explanation for the curvature observed in our data is that the higher concentration data was collected in a regime where the air was relatively immune to losses by either wet or dry deposition.

Such conditions would cause (as observed) unusually high retention of  $\text{NO}_x$  oxidation products leading to the observation of a slope lower than would be measured under conditions where such losses were significant (e.g., surface measurements over land, or in air that had been subjected to wet deposition losses). Whether retention is the principal cause of the change in slope of the  $\text{O}_3$ - $\text{NO}_z$  plot with  $\text{NO}_z$  concentration is uncertain. However, this possibility clearly points out the need to adequately account for physical losses of  $\text{NO}_z$  from the atmosphere when inferring  $\text{O}_3$  production from analysis of  $\text{O}_3$ - $\text{NO}_z$  plots.

**Correlation of  $\text{O}_3$  with  $(\text{NO}_z + 2\text{H}_2\text{O}_2)$ .** Correlation of the quantity  $(\text{NO}_z + 2\text{H}_2\text{O}_2)$  with  $\text{O}_3$  is suggested by calculations and a similar plot of modeled concentrations by Sillman 1995. The sense of this correlation may be best understood in the context of radical sources and sinks. In this view, the quantity  $(\text{NO}_z + 2\text{H}_2\text{O}_2)$  represents, approximately, the cumulative radical sink since the air mass had last been cleansed of soluble oxidation products (e.g.,  $\text{HNO}_3$  and  $\text{H}_2\text{O}_2$ ). The  $\text{H}_2\text{O}_2$  concentration is multiplied by 2 in this formulation because two radicals are consumed in formation of each molecule of peroxide. The  $\text{O}_3$  concentration is a measure of radical source strength of an air mass because  $\text{O}_3$  photolysis and subsequent reaction of  $\text{O}(^1\text{D})$  with  $\text{H}_2\text{O}$  is the principal source of radicals in the atmosphere. It is understood that an exact accounting of radical sources and sinks would include, for example,  $\text{HCHO}$  photolysis as a source and reaction of  $\text{H}_2\text{O}_2$  with  $\text{OH}$  as a sink of radicals, but for a first approximation these processes are ignored.

A plot of the quantity  $(\text{NO}_z + 2\text{H}_2\text{O}_2)$  versus the  $\text{O}_3$  concentration for the NARE plume data is shown in Figure 10. The plot exhibits a linear increase in  $(\text{NO}_z + 2\text{H}_2\text{O}_2)$  with  $\text{O}_3$ , with a slope of 0.22, an intercept of -2.2, and an  $r^2=0.73$  (calculated from the individual data points). The correlation between  $\text{O}_3$  and  $(\text{NO}_z + 2\text{H}_2\text{O}_2)$  is much better than the correlation between  $\text{O}_3$  and  $\text{H}_2\text{O}_2$  ( $r^2 = 0.43$ ), and marginally better than the correlation between  $\text{O}_3$  and  $\text{NO}_z$  ( $r^2 = 0.68$ ). As shown above, the relationship between  $\text{O}_3$  and  $\text{NO}_z$  is not even linear, exhibiting

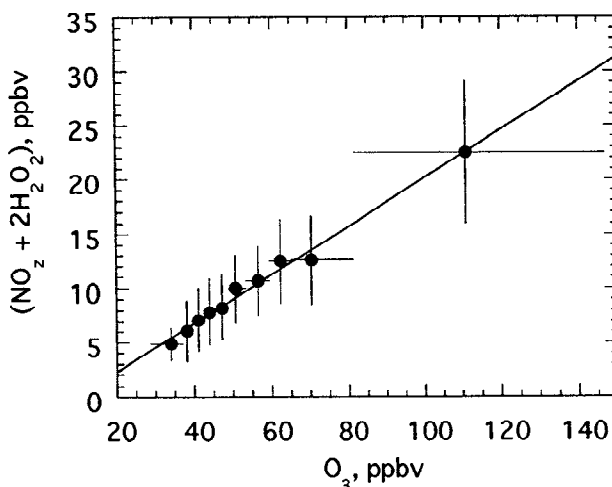


**Figure 10.** Binned  $(\text{NO}_z + 2\text{H}_2\text{O}_2)$  concentration as a function of the binned  $\text{O}_3$  concentration. Sixty-second data were ordered by  $(\text{NO}_z + 2\text{H}_2\text{O}_2)$  concentration and divided into 10 intervals. Each point on the plot represents the average  $(\text{NO}_z + 2\text{H}_2\text{O}_2)$  and  $\text{O}_3$  concentration for the intervals. Horizontal bars represent the range of  $\text{O}_3$  concentration for the interval; vertical bars represent the standard deviation of the  $(\text{NO}_z + 2\text{H}_2\text{O}_2)$  concentration for the interval. Slope and intercept were calculated from the individual data points

two distinct slopes corresponding to low and high  $\text{NO}_x$  concentrations; a similar nonlinearity between  $\text{O}_3$  and  $\text{NO}_x$  is exhibited by the model calculations of Sillman [1995].

In some respects, it is not surprising that the correlation between  $(\text{NO}_x + 2 \text{H}_2\text{O}_2)$  and  $\text{O}_3$  is better than the correlation between  $\text{O}_3$  and either  $\text{H}_2\text{O}_2$  or  $\text{NO}_x$  considering the fairly large range of conditions and air mass ages that our measurements encompass, and what that implies about how radicals are lost from the atmosphere. Early in the photochemical life of an air mass,  $\text{NO}_y$  will primarily be in the form of  $\text{NO}_x$ , and radicals will be lost mainly by reaction of OH with  $\text{NO}_2$  to form nitric acid; little peroxide will be formed, and significant correlation between  $\text{O}_3$  and  $\text{H}_2\text{O}_2$  would not be expected. As the air mass ages and the  $\text{NO}_x$  concentration decreases through formation of  $\text{HNO}_3$ , more radicals will be lost from the system through formation of peroxides [Kleinman, 1986; 1991] and the number of  $\text{O}_3$  molecules generated per molecule of  $\text{NO}_x$  converted to  $\text{NO}_2$  will increase [Liu et al., 1987]. When  $\text{NO}_x$  reaches very low values peroxide formation will be the dominant radical sink and should be well correlated with the  $\text{O}_3$ .

By plotting  $\text{O}_3$  versus  $(\text{NO}_x + 2 \text{H}_2\text{O}_2)$  we are including both conditions when formation of  $\text{NO}_x$  (principally  $\text{HNO}_3$ ) is the principal radical sink and conditions when peroxides are the principal radical sink and focusing not on  $\text{O}_3$  formation, but on the role of  $\text{O}_3$  as a radical source. That the relationship between  $\text{O}_3$  and  $(\text{NO}_x + 2 \text{H}_2\text{O}_2)$  is strong, is probably due to several factors. First, the sampled air masses had not been in contact with source regions for periods of up to several days, and thus the complicating effects of addition of fresh quantities of  $\text{NO}_x$  and/or hydrocarbons were avoided. Second, measurements were made under conditions such that the radical sink species (principally,  $\text{HNO}_3$  and  $\text{H}_2\text{O}_2$ ) were retained by the air mass, having not been lost by either wet or dry deposition processes or chemistry. Such losses would have destroyed the observed correlation. Third, the air masses were aged to the point that significant peroxide had been formed, but not to the point that such formation involved consumption of  $\text{O}_3$ .

#### 4. Summary and Conclusions

Plumes of anthropogenic pollutants transported distances up to 1000 km downwind of source regions in the northeastern United States were sampled over the WNAO during late summer 1993. For the most part these plumes were observed in well defined layers at altitudes between 0.3 and 2 km above the surface. On several days, plumes were found to extend over distances in excess of 250 km, and to be as much as 1000 m thick. Because of the mode of transport, and because conditions were generally dry when plumes were advected off the east coast of North America, the chemical species contained in these plumes were not subject to losses to the surface by either dry or wet deposition processes. This led to unusually high accumulation of photochemical oxidation products.

The composition of these plumes was characteristic of air masses combined with substantial quantities of anthropogenic pollutants which had been processed photochemically.  $\text{O}_3$  concentrations as high as 150 ppbv were measured. High  $\text{O}_3$  concentrations were associated with CO concentrations of up to 480 ppbv,  $\text{NO}_y$  concentrations up to 20 ppbv, and accumulation mode particle number densities of the order of 2000–3000  $\text{cm}^{-3}$ . Aerosol composition measurements indicated that the aerosol was composed principally of acidic sulfate; aerosol nitrate and chloride represented only a small fraction of the mass. Accumulation mode particle number densities were reasonably well correlated ( $r^2=0.64$ ) with the aerosol-S mass concentration.

$\text{NO}_y$  was predominantly composed of  $\text{NO}_x$  oxidation products;  $\text{NO}_x$  concentrations represented only a small fraction of the total  $\text{NO}_y$  ( $\leq 16\%$ ); t- $\text{NO}_3$  was found to be the principal product species representing, on average, 70% of the  $\text{NO}_y$ .  $\text{H}_2\text{O}_2$  concentrations were quite high, averaging nearly 4 ppbv, and exhibiting a maximum concentration in excess of 11 ppbv. The high t- $\text{NO}_3$  and  $\text{H}_2\text{O}_2$  concentrations in conjunction with high  $\text{O}_3$  concentrations indicate that the plumes had undergone extensive processing in transit from source regions to the sampling locations, and were well aged photochemically.

Significant correlation between the concentrations of various species were found. Good correlation were observed between CO and  $\text{O}_3$ , CO and particle number densities, and CO and  $\text{NO}_y$ . The slope of the CO versus  $\text{O}_3$  curve was similar to values measured previously at the surface in the project area [Parrish, 1993a].  $\text{O}_3$  was found to depend nonlinearly on both the  $\text{NO}_y$  and  $\text{NO}_x$  concentrations. At low concentrations the slope was within the range of values measured previously in photochemically aged air masses in the eastern United States. At high  $\text{NO}_y/\text{NO}_x$  concentrations the slope was a factor of 2 or more lower than has previously been observed in aged air masses. The low slope was attributed either to the variation in efficiency of  $\text{O}_3$  production with  $\text{NO}_x$  concentration as predicted by models [Liu et al., 1987], or to the retention of an unusually high fraction of  $\text{NO}_x$  oxidation products in these plumes in comparison to other observations.

A strong linear correlation was found between the concentration of radical sink species as represented by the quantity  $(\text{NO}_x + 2 \text{H}_2\text{O}_2)$  and  $\text{O}_3$ . This correlation links the correlation between  $\text{O}_3$  and  $\text{NO}_x$ , and  $\text{O}_3$  and  $\text{H}_2\text{O}_2$ , and emphasizes the role of  $\text{O}_3$  as the principal (but not sole) source of radicals in the atmosphere.

**Acknowledgments.** The authors gratefully acknowledge R. Hannigan and M. Warren of the Battelle Pacific Northwest Laboratory for piloting the aircraft, Stephen Springston and Linda Nunermacker for preparing the instrumentation, Sanford Sillman for helpful discussions during analysis of the data, and the Atmospheric Environment Service of Canada for providing meteorological forecasts. This research was performed under sponsorship of the United States Department of Energy under contracts DE-AC02-76CH00016.

#### References

- Anderson, B. E., et al., The impact of United States continental outflow on ozone and aerosol distributions over the western N. Atlantic, *J. Geophys. Res.*, 98, 23,477–23,489, 1993.
- Berkowitz, C. M., P. H. Daum, C. Spicer, and K. M. Busness, Synoptic patterns associated with the flux of excess ozone to the western North Atlantic, *J. Geophys. Res.*, this issue.
- Boatman, J. F., et al., Airborne sampling of selected trace chemicals above the central United States, *J. Geophys. Res.*, 94, 5081–5093, 1989.
- Buhr, M. P., D. M. Parrish, R. B. Norton, F. C. Fehsenfeld, R. E. Sievers, and J. M. Roberts, Contribution of organic nitrates to the total reactive nitrogen budget at a rural eastern United States site, *J. Geophys. Res.*, 95, 9809–9816, 1990.
- Carroll, M. A., et al., Measurements of Nitric Oxide and nitrogen dioxide during the Mauna Loa observatory photochemistry experiment, *J. Geophys. Res.*, 97, 10,361–10,374, 1992.
- Charlson, R. J., J. Langner, H. Rodhe, C. B. Leovy, and S. G. Warren, Perturbation of the northern hemisphere radiative balance by backscattering from anthropogenic sulfate aerosols, *Tellus*, 43, 152–163, 1991.
- Chin, M., D. J. Jacob, J. W. Munger, D. D. Parrish, and Doddridge B. G., Relationship of ozone and carbon monoxide over North America, *J. Geophys. Res.*, 99, 14,565–14,573, 1994.
- Daum, P. H., et al., Winter measurements of trace gas and aerosol composition at a rural site in southern Ontario, *Atmos. Environ.*, 23, 161–173, 1989.
- Daum, P. H., et al., Measurement and interpretation of concentrations

- of  $\text{H}_2\text{O}_2$  and related species in the upper Midwest during summer, *J. Geophys. Res.*, **95**, 9857-9871, 1990.
- Daum, P. H., and D. F. Leahy, The Brookhaven National Laboratory filter pack sampling system for collection and determination of air pollutants, Rep. BNL-31381, Brookhaven Natl. Lab., Upton, NY, 1985.
- Dickerson, R. R., and A. C. Delaney, Modification of a commercial gas filter correlation CO detector for enhanced sensitivity, *J. Atmos. Ocean. Technol.*, **5**, 424-431, 1988.
- Doddridge, B. G., R. R. Dickerson, R. G. Wardell, K. L. Civerolo, and L. J. Nunnermacker, Trace gas concentrations and meteorology in rural Virginia, 2, Reactive nitrogen compounds, *J. Geophys. Res.*, **97**, 20,631-20,646, 1992.
- Fishman, J., F. W. Vukovich, and E. V. Browell, The photochemistry of synoptic-scale ozone synthesis: Implications for the global tropospheric ozone budget, *J. Atmos. Chem.*, **3**, 299-320, 1985.
- Galloway, J. N., D. M. Whelpdale, and G. T. Wolff, The flux of S and N eastward from North America, *Atmos. Environ.*, **18**, 2595-2607, 1984.
- Heikes, B. G., J. G. Walega, G. L. Kok, J. G. Walega, and A. L. Lazrus,  $\text{H}_2\text{O}_2$ ,  $\text{O}_3$  and  $\text{SO}_2$  measurements in the lower troposphere over the eastern United States during fall, *J. Geophys. Res.*, **92**, 915-931, 1987.
- Hellpointer, E., and S. Gab, Detection of methyl, hydroxymethyl and hydroxyethylperoxides in air and precipitation, *Nature*, **337**, 631-634, 1989.
- Hewitt, C. N., and G. L. Kok, Formation and Occurrence of organic hydroperoxides in the troposphere: Laboratory and field observations, *J. Atmos. Chem.*, **12**, 181-194, 1991.
- Isaksen, I. S. A., and P. Hov, Calculation of trends in the tropospheric concentration of  $\text{O}_3$ , OH, CO,  $\text{CH}_4$  and  $\text{NO}_x$ , *Tellus*, **39B**, 271-285, 1987.
- Kleinman, L. I., Photochemical formation of peroxides in the boundary layer, *J. Geophys. Res.*, **91**, 10,889-10,904, 1986.
- Kleinman, L. I., Seasonal dependence of boundary layer peroxide concentration: The low and high  $\text{NO}_x$  regimes, *J. Geophys. Res.*, **96**, 20,721-20,733, 1991.
- Kleinman, L. I., et al., Ozone formation at a rural site in the southeastern United States, *J. Geophys. Res.*, **99**, 3469-3482, 1994.
- Lazrus, A. L., G. L. Kok, S. Gitlin, and J. A. Lind, An automated fluorometric method for hydrogen peroxide in atmospheric precipitation, *Anal. Chem.*, **57**, 917-922, 1985.
- Lee, J. H., D. F. Leahy, I. N. Tang, and L. Newman, Measurement and speciation of gas phase peroxides in the atmosphere, *J. Geophys. Res.*, **98**, 2911-2915, 1993.
- Lee, J. H., I. N. Tang, and J. B. Weinstein-Lloyd, Non-enzymatic method for the determination of hydrogen peroxide in atmospheric samples, *Anal. Chem.*, **62**, 2381-2384, 1990.
- Lee, J. H., I. N. Tang, J. B. Weinstein-Lloyd, and E. B. Halper, Improved non-enzymatic method for determination of gas-phase peroxide, *Environ. Sci. Technol.*, **28**, 1180-1185, 1994.
- Lin, X., M. Trainer, and S. C. Liu, On the nonlinearity of tropospheric ozone production, *J. Geophys. Res.*, **93**, 15,879-15,888, 1988.
- Liu, S. C., et al., Ozone production in the rural troposphere and the implications for regional and global ozone distributions, *J. Geophys. Res.*, **92**, 4191-4207, 1987.
- Mauzerall, D. L., et al., An ozone budget for the remote troposphere over eastern Canada, *Eos Trans. AGU*, **74**(43), Fall Meeting Supp. 1, 180, 1993.
- Olszyna, K. J., E. M. Bailey, R. Simonaitis, and J. F. Meagher,  $\text{O}_3$  and  $\text{NO}_x$  relationships at a rural site, *J. Geophys. Res.*, **99**, 14,557-14,563, 1994.
- Parrish, D. D., J. S. Holloway, M. Trainer, P. C. Murphy, G. L. Forbes, and F. C. Fehsenfeld, Export of North American ozone pollution to the North Atlantic Ocean, *Science*, **259**, 1436-1439, 1993a.
- Parrish, D. D., et al., The total reactive oxidized nitrogen levels and the partitioning between the individual species at six rural sites in eastern North America, *J. Geophys. Res.*, **98**, 2927-2939, 1993b.
- Schwartz, S. E., Are global cloud albedo and climate controlled by marine phytoplankton?, *Nature*, **341**, 441-445, 1988.
- Sillman, S., The use of  $\text{NO}_x$ , HCHO,  $\text{H}_2\text{O}_2$  and  $\text{HNO}_3$  as empirical indicators for Ozone- $\text{NO}_x$ -ROG sensitivity in urban locations, *J. Geophys. Res.*, **100**, 14,175-14,188, 1995.
- Spicer, C. W., D. V. Kenny, W. J. Shaw, K. M. Busness, and E. G. Chapman, A laboratory in the sky: New frontiers in measurements aloft, *Environ. Sci. Technol.*, **28**, 412A-420A, 1994.
- Thompson, A. M., R. W. Stewart, M. A. Owens, and J. A. Herwehe, Sensitivity of tropospheric oxidants to global chemical and climate change, *Atmos. Environ.*, **23**, 519-532, 1989.
- Trainer, M., et al., Observations and modeling of the reactive nitrogen photochemistry at a rural site, *J. Geophys. Res.*, **96**, 3045-3062, 1991.
- Trainer, M. et al., Correlation of ozone with  $\text{NO}_x$  in photochemically aged air, *J. Geophys. Res.*, **98**, 2917-2925, 1993.
- Weinstein-Lloyd, J., P. H. Daum, J. H. Lee, L. J. Nunnermacker, and L. Kleinman, Measurement of peroxides and related species in the 1993 North Atlantic Regional Experiment, *J. Geophys. Res.*, this issue.
- Zaucker, F., P. H. Daum, U. Wegner, C. Berkowitz, B. Kromer, and W. S. Broecker, Atmospheric  $^{222}\text{Rn}$  measurements during the 1993 NARE intensive, *J. Geophys. Res.*, this issue.

P. H. Daum, L. I. Kleinman, and L. Newman, Brookhaven National Laboratory, Department of Applied Science, Environmental Chemistry Division, Upton, NY 11973-5000. (e-mail: phdaum@bnlux1.bnl.gov; kleinman@bnlcl6.bnl.gov; newman@bnl.gov)

J. B. Weinstein-Lloyd, Chemistry and Physics Department, SUNY/Old Westbury, Old Westbury, NY 11568-0210. (e-mail: jlloyd@bnl.gov)

C. M. Berkowitz and K. M. Busness, Battelle Pacific Northwest Laboratory, P.O. Box 9999, Richland, WA 99352. (e-mail: cm\_berkowitz@pnl.gov; km\_busness@pnl.gov).

(Received April 14, 1995; revised August 30, 1995; accepted August 30, 1995.)